Polymerization of Lactide by Monomeric Sn(II) Alkoxide Complexes

Katherine B. Aubrecht, Marc A. Hillmyer,* and William B. Tolman*

Department of Chemistry, University of Minnesota, 207 Pleasant St. SE, Minneapolis, Minnesota 55455-0431

Received October 29, 2001

ABSTRACT: Monomeric Sn(II) alkoxide complexes of bulky amidinate ligands *N*,*N*′-bis(trimethylsilyl)-benzamidinate, $[L^{SiMe3}]^-$, and *N*,*N*′-bis(dimethylphenylsilyl)benzamidinate, $[L^{SiMe2Ph}]^-$, and the corresponding bis(amidinate) compounds were synthesized and structurally characterized by single-crystal X-ray diffraction. The monomeric nature of these complexes in the solid state was retained in solution as evinced by NMR spectroscopy. Both alkoxide complexes were active for DL-lactide (LA) polymerization in toluene solution at 80 °C. The controlled polymerization of LA by $L^{SiMe2Ph}Sn(OCPh_3)$ was observed in the presence of 1.0 equiv of an exogenous alcohol. Under these conditions, the polymerization reaction was found to be first order in [LA] and about one-third order in $[L^{SiMe2Ph}Sn(OCPh_3)]_0$. The polymerization kinetics were further analyzed by applying a model that invokes aggregation of the active species, with one inactive, aggregated form and one active, unaggregated form. The importance of aggregation in understanding catalyst reactivity is highlighted.

Introduction

An effective preparative route to a variety of useful polyester thermoplastics is the metal-mediated ring-opening polymerization of cyclic esters. This synthetic method can enable control of polymer molecular weight and backbone stereochemistry and can yield macromolecular samples with narrow molecular weight distributions. Such tuning of polymerization reaction behavior is important to achieve because of the intimate relationship between molecular characteristics and material properties. Efforts toward this goal have been extensive[1] for polylactide (PLA), a key member of the polyester class that has garnered special interest because it is a biodegradable polymer derived from the ring-opening polymerization of lactide, a renewable resource.[2,3] PLA-based products have been available for several decades in a variety of biomedical products (e.g., resorbable sutures), and the full-scale production of PLA was announced recently.[4]

The most widely used catalyst for the ring-opening polymerization of lactide is Sn(II) 2-ethylhexanoate, Sn(Oct)$_2$.[5] Recently reported studies of the mechanism of Sn(Oct)$_2$-mediated polymerizations of lactide at 80 °C in the presence of an added alcohol (or fortuitous hydroxyl-containing impurities in the feed) have shown that the active species is a Sn(II) alkoxide.[6−8] Independently prepared Sn(OBu)$_2$ also is an effective catalyst, although it exists as a number of aggregates in solution.[9] The aggregation of catalyst and/or of metal-capped polymer chains creates multiple catalytic species and can complicate the interpretation of kinetic data. Single-site catalysts offer the promise of mechanistic simplicity and amenability to reactivity control through ligand design. A useful strategy toward single-site systems involves incorporation of bulky ligands that inhibit oligomerization of the metal complex through steric interactions. While homoleptic Sn(II) complexes (containing only one type of ligand) of less hindered alkoxides such as methoxide and ethoxide have polymeric solid-state structures,[10] bulky alkoxides such as 2,6-di-*tert*-butylaryl oxide yield monomeric Sn(OR)$_2$ compounds.[11,12] Recently, a monomeric Sn(II) catalyst for lactide polymerization was reported using a hindered β-diketiminate as a supporting ligand, and it exhibited good activity for the controlled polymerization of lactide.[13]

Our efforts have focused on obtaining similar species, but with sterically hindered, bidentate benzamidinates as ancillary ligands.[14−18] Here, we report the synthesis and characterization of several new monomeric LSn(II)OR compounds comprising bulky benzamidinate (L) and alkoxide ligands. We then describe studies of their lactide polymerization activity, including kinetic studies that reveal important information about the nature of the active catalytic species.

Results and Discussion

Synthesis and Characterization of Sn Complexes. The target LSnOR complexes were prepared using the synthetic strategy illustrated in Schemes 1 and 2. Treatment of a THF solution of the sodium benzamidinate $Na[L^{SiMe3}](OEt_2)$[19] sequentially with 1.0 equiv of $SnCl_2$ and 1.0 equiv of lithium hexamethyldisilazide (LiHMDS) gave the intermediate $L^{SiMe3}Sn[N(SiMe_3)_2]$, which was isolated as a viscous oil, characterized by ^{1}H NMR spectroscopy, and then used without further purification. Reaction of $L^{SiMe3}Sn[N(SiMe_3)_2]$ with 1.0 equiv of Ph_3COH yielded $L^{SiMe3}Sn(OCPh_3)$ as colorless blocks upon crystallization at −35 °C. A previously unreported, more hindered benzamidinate ligand $[L^{SiMe2Ph}]^-$ was synthesized by treating $(PhSiMe_2)_2NLi$ with benzonitrile and TMEDA (Scheme 2). The resulting lithium amidinate, $Li[L^{SiMe2Ph}](TMEDA)$, was treated sequentially with $SnCl_2$, LiHMDS, and Ph_3COH to obtain $(L^{SiMe2Ph})Sn(OCPh_3)$. Both compounds $LSn(OCPh_3)$ ($L = L^{SiMe3}$ and $L^{SiMe2Ph}$) were characterized in the solid state by X-ray crystallography and elemental analysis and in solution by NMR methods. The use of smaller alcohols (e.g., $PhCH_2OH$, Ph_2CHOH, $Me_2NCH_2CH_2OH$) in analogous preparative protocols did not lead to LSnOR species; instead, the bis(amidinate) complexes $(L^{SiMe2Ph})_2Sn$ and $(L^{SiMe3})_2Sn$

* To whom correspondence should be addressed: E-mail hillmyer@chem.umn.edu or tolman@chem.umn.edu.

10.1021/ma011873w CCC: $22.00
Published on Web 01/03/2002

Scheme 1

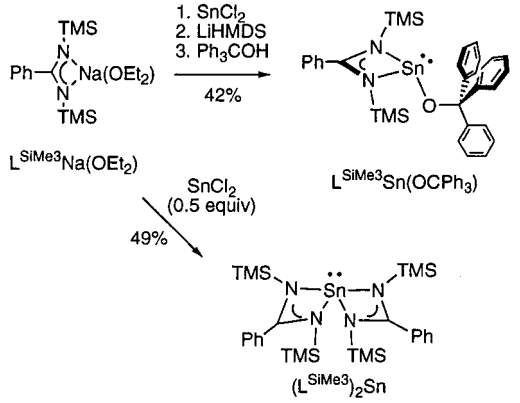

Scheme 2

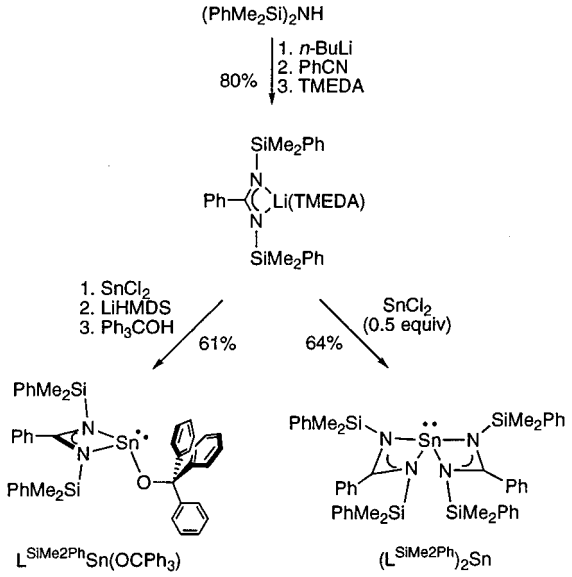

were the only compounds isolated. To corroborate their identity, these bis(amidinate) compounds were prepared and characterized independently using 1.0 equiv of $SnCl_2$ and 2.0 equiv of the corresponding amidinate anions.

X-ray diffraction data for $LSn(OCPh_3)$ ($L = L^{SiMe3}$ and $L^{SiMe2Ph}$) are listed in Table 1. The structures of $LSn(OCPh_3)$ are shown in Figures 1 and 2, while those of L_2Sn appear in Figures S1 and S2. The monomeric, 3-coordinate alkoxide complexes both display a distorted pyramidal geometry clearly indicative of a stereochemically active lone pair. The structures of the two alkoxide complexes differ little from each other, suggesting that the two amidinate ligands have similar steric influences despite their different substituents. The bis(amidinate) compounds exhibit structures similar to those of other reported Sn(II) complexes of this type.[16,18]

Solution NMR data revealed important structural information relevant to understanding polymerization catalysis. The ^{119}Sn NMR spectra (d_6-benzene) of the complexes $L^{SiMe3}Sn(OCPh_3)$ and $L^{SiMe2Ph}Sn(OCPh_3)$ displayed a single resonance at −54.2 and −70.3 ppm, respectively. The bis(amidinate) compounds also exhibited a singlet, but at −244.6 ppm for $(L^{SiMe3})_2Sn$ and at −227.0 ppm for $(L^{SiMe2Ph})_2Sn$, significantly upfield of the alkoxide complex signals. Importantly, single resonances at relatively constant chemical shifts were observed for the alkoxide complexes over the concentration range 0.01−0.1 M and from 25 to 80 °C. These data

Table 1. Summary of X-ray Crystallographic Data for $L^{SiMe3}Sn(OCPh_3)$ and $L^{SiMe2Ph}Sn(OCPh_3)$

empirical formula	$C_{32}H_{38}N_2OSi_2Sn$	$C_{42}H_{42}N_2OSi_2Sn$
formula weight	641.51	765.65
crystal system	triclinic	monoclinic
space group	$P\bar{1}$	$P2_1/n$
a (Å)	12.2022 (8)	9.0251 (7)
b (Å)	10.6095 (7)	20.1215 (15)
c (Å)	14.6587 (10)	20.8081 (16)
α (deg)	78.5980 (10)	90
β (deg)	66.0920 (10)	92.930 (2)
γ (deg)	67.0110 (10)	90
V (Å^3)	1595.33 (18)	3773.8 (5)
Z	2	4
density (calcd) (g/cm^3)	1.335	1.348
crystal size (mm)	0.4 × 0.2 × 0.2	0.5 × 0.25 × 0.2
absorption coeff	0.902 mm^{-1}	0.775 mm^{-1}
2θ max (deg)	54.94	55.06
no. of reflns colld	9650	23164
no. of ind reflns	6899	8446
no. of obsd reflns [$I > 2\sigma(I)$]	6467	7174
params	349	437
$R1^a$ [$I > 2\sigma(I)$]	0.0278	0.0287
$wR2^b$	0.0686	0.0747
goodness-of-fit	1.144	1.026
largest diff peak and hole (e$^-$ Å^{-3})	0.626, −0.662	0.640, −0.413

^{a} $R1 = \sum||F_o| - |F_d||/\sum|F_o|$. ^{b} $wR2 = [\sum[w(F_o^2 - F_c^2)^2]/[\sum[w(F_o^2)^2]]^{1/2}$, where $w = 1/\sigma^2(F_o^2) + (aP)^2 + bP$.

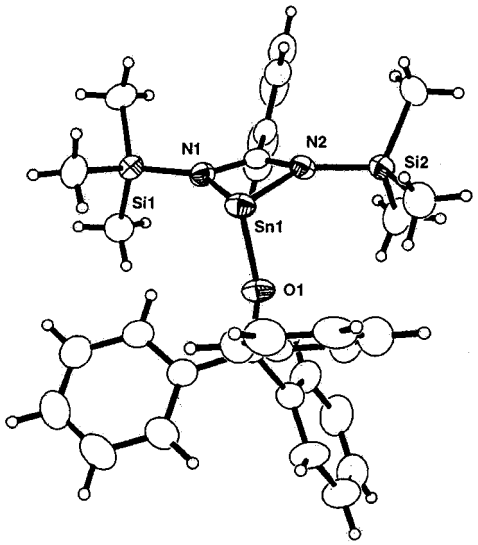

Figure 1. Representation of the X-ray crystal structure of $L^{SiMe3}Sn(OCPh_3)$, with all atoms shown as 50% thermal ellipsoids. Selected distances (Å) and angles (deg): Sn(1)−N(1), 2.251(2); Sn(1)−N(2), 2.224(2); Sn(1)−O(1), 2.039(2); N(1)−Sn(1)−N(2), 60.48(6); O(1)−Sn(1)−N(1), 90.55(6); O(1)−Sn(1)−N(2), 87.27(6).

show that redistribution of ligands[20] or change in aggregation state does not occur under typical conditions used for polymerizations described below.[21] The ^1H NMR data are generally consistent with the structures determined by X-ray diffraction. Thus, $L^{SiMe3}Sn(OCPh_3)$, and $(L^{SiMe3})_2Sn$ each display a single $-CH_3$ peak at room temperature, and $(L^{SiMe2Ph})Sn(OCPh_3)$ displays two $-CH_3$ peaks (δ 0.084, 0.043 ppm) that do not vary between room temperature and 90 °C, indicating that the methyl groups on each Si atom remain diastereotopic.

Lactide Polymerization Activity and Selectivity. The two monomeric Sn(II) alkoxides are effective for the polymerization of DL-lactide (LA) in toluene solution at

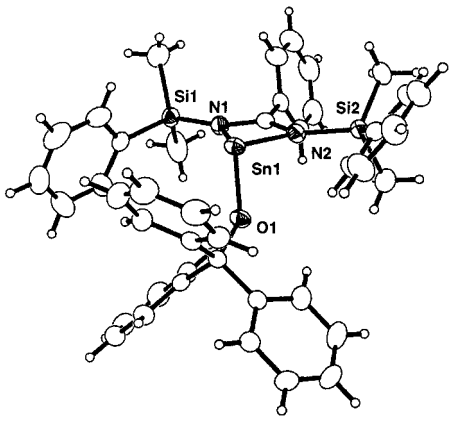

Figure 2. Representation of the X-ray crystal structure of $L^{SiMe2Ph}Sn(OCPh_3)$, with all atoms shown as 50% thermal ellipsoids. Selected distances (Å) and angles (deg): Sn(1)−N(1), 2.248(2); Sn(1)−N(2), 2.253(2); Sn(1)−O(1), 2.036(1); N(1)−Sn(1)−N(2), 60.07(6); O(1)−Sn(1)−N(1), 94.76(6); O(1)−Sn(1)−N(2), 88.65(5).

80 °C, conditions typically utilized for the solution polymerization of lactide and related cyclic esters.[1] For comparison purposes we focused on these conditions, and while some optimization experiments were carried out, a thorough optimization of the temperature and solvents has not been performed. For example, using $[LA]_0 = 1.0$ M and a ratio $[LA]_0/[L^{SiMe3}Sn(OCPh_3)]_0$ of 450, we observed 93% conversion of LA in 35 min. The resulting PLA had a $M_n = 63.5$ kg/mol and a polydispersity index (PDI) of 1.48. Using $L^{SiMe2Ph}Sn(OCPh_3)$ under similar conditions ($[LA]_0/[L^{SiMe2Ph}Sn(OCPh_3)]_0 = 500$), 92% conversion of LA in 165 min gave a PLA sample with $M_n = 28.9$ kg/mol and PDI = 1.18. While the somewhat smaller $L^{SiMe3}Sn(OCPh_3)$ exhibited moderate control over molecular weight, we focus the remaining discussion on the polymerization of lactide using $L^{SiMe2Ph}Sn(OCPh_3)$ because at similar conversions of lactide, the PLA obtained using this compound generally displayed a lower PDI than the PLA obtained using $L^{SiMe3}Sn(OCPh_3)$.

We investigated the M_n of the PLA produced using $L^{SiMe2Ph}Sn(OCPh_3)$ as a function of LA conversion and observed a linear relationship ($[LA]_0/[L^{SiMe2Ph}Sn(OCPh_3)]_0 = 300$, $[LA]_0 = 1.0$ M, toluene, 80 °C). The PDI values of the PLA products we obtained were between 1.16 and 1.43. Although these data are consistent with a controlled polymerization, we noticed that while different batches of LA gave similarly controlled behavior, the actual values for M_n were variable at constant $[LA]_0/[L^{SiMe2Ph}Sn(OCPh_3)]_0$ and LA conversion. This lack of reproducibility suggests that fortuitous initiators in the LA feed may be interfering with the initiation when $L^{SiMe2Ph}Sn(OCPh_3)$ is used. Furthermore, by ^{1}H NMR spectroscopy, we observed $-OCPh_3$ end groups in these polymerizations, but M_n determinations using integration of these end groups relative to the polymer backbone were not consistent with values of M_n calculated by stoichiometry and yield considerations. One liability of using bulky initiators such as $L^{SiMe2Ph}Sn(OCPh_3)$ is the possibility of sluggish initiation of the polymerization due to steric congestion around the metal center. Given these results, we chose to examine the polymerization efficacy of $L^{SiMe2Ph}Sn(OCPh_3)$ in the presence of benzyl alcohol (BnOH) as an added initiator.[22]

Polymerizations of LA effected by $L^{SiMe2Ph}Sn(OCPh_3)$ in the presence of 1.0 equiv of BnOH display good

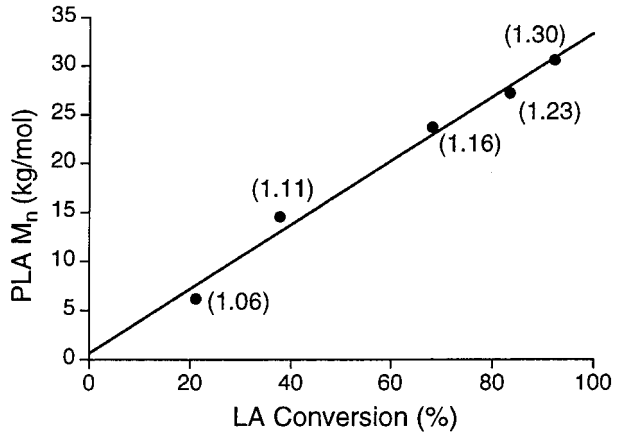

Figure 3. Plot of PLA M_n (kg/mol) as a function of conversion for polymerization of DL-lactide by $L^{SiMe2Ph}Sn(OCPh_3)$ with added BnOH. Polymerization conditions: $[LA]_0/[L^{SiMe2Ph}Sn(OCPh_3)]_0 = 200$, $[L^{SiMe2Ph}Sn(OCPh_3)]_0/[BnOH]_0 = 1$, $[LA]_0 = 1.0$ M, toluene, 80 °C. Values of M_w/M_n (PDI) are indicated in parentheses next to the data points.

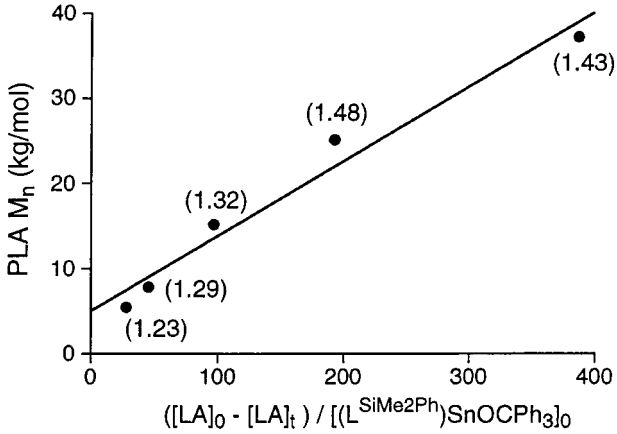

Figure 4. Plot of PLA M_n (kg/mol) as a function $[LA]_0/[L^{SiMe2Ph}Sn(OCPh_3)]_0$ for polymerization of DL-lactide by $L^{SiMe2Ph}Sn(OCPh_3)$ with added BnOH. Polymerization conditions: $[L^{SiMe2Ph}Sn(OCPh_3)]_0/[BnOH]_0 = 1$, $[LA]_0 = 1.0$ M, toluene, 80 °C. All polymerizations were stopped and sampled at >90% conversion. M_w/M_n (PDI) values are indicated in parentheses next to the data points.

control as evinced by (1) a linear increase in PLA M_n as a function of LA conversion (Figure 3), (2) observation of narrow polydispersities up to 80% conversion of LA (Figure 3), and (3) a linear increase in PLA M_n as a function of the ratio of converted monomer to initial catalyst (Figure 4). Additionally, in a test of the living character of the polymerization LA (50 equiv) was polymerized to 85% conversion (20 min) using $L^{SiMe2Ph}Sn(OCPh_3)$ with 1.0 equiv of BnOH to yield PLA with $M_n = 9.62$ kg/mol and PDI = 1.12. A second portion of LA (300 equiv) was then added, and the polymerization of this lot proceeded to 94% conversion in 90 min to yield PLA with $M_n = 33.9$ kg/mol and PDI = 1.62. Nevertheless, termination of active chains was observed, as indicated by a slight low-molecular-weight feature in the SEC trace that presumably corresponds to "dead" polymer chains from the initial polymerization. The complex $L^{SiMe2Ph}Sn(OCPh_3)$ with 1.0 equiv of BnOH also is an active catalyst system for the melt polymerization of neat LA; heating 200 equiv of LA to 120 °C for 20 min afforded PLA in 97% yield with $M_n = 20.2$ kg/mol and PDI = 2.40.

To probe the nature of the initiating species in these polymerizations mediated by $L^{SiMe2Ph}Sn(OCPh_3)$ with added alcohol, ^1H NMR analysis of polymer end groups was performed. To obviate complications in the analysis due to overlapping resonances observed when using BnOH, we used EtOH as the exogenous alcohol in these experiments. As mentioned above, PLA prepared using only $L^{SiMe2Ph}Sn(OCPh_3)$ displayed $-OCPh_3$ end group resonances in the ^1H NMR spectrum. However, the intensity ratio of resonances of the PLA backbone to the $-OCPh_3$ groups gave values that were much higher (e.g., by a factor of 3) than expected from the $([LA]_t - [LA]_0)/[L^{SiMe2Ph}Sn(OCPh_3)]_0$ ratio. We were unable to observe any other end groups (initiating or terminating). These results indicate that only a fraction of the original $L^{SiMe2Ph}Sn(OCPh_3)$ molecules may be initiating the polymerization. On the other hand, in the presence of EtOH, both $-OEt$ and $-OCPh_3$ end groups were clearly visible in the ^1H NMR spectrum, and the integration of these peaks gave values more consistent with those expected on the basis of both the $([LA]_t - [LA]_0)/[L^{SiMe2Ph}Sn(OCPh_3)]_0$ and $([LA]_t - [LA]_0)/[EtOH]_0$ ratios. From these results, not only does the added EtOH (and by analogy, BnOH) effectively initiate the polymerization, but it also appears to enhance the initiation efficiency of the Sn(II) reagent.

Polymerizations of LA using $L^{SiMe2Ph}Sn(OCPh_3)$ or $L^{SiMe3}Sn(OCPh_3)$ alone or $L^{SiMe2Ph}Sn(OCPh_3)$ in combination with BnOH in toluene at 80 °C yield PLA with a slight heterotactic bias.[23] The methine region of the homonuclearly decoupled ^1H NMR spectrum displays a decrease in the intensity of the resonance of the iii (or mmm) tetrad at 5.172 ppm relative to that of atactic PLA (Figure S3). On the other hand, PLA made using $L^{SiMe2Ph}Sn(OCPh_3)$/BnOH in the melt is completely atactic. Thus, the high level of chain-end stereocontrol demonstrated by recently reported[24] $[LZnOR]_2$ (L = bulky β-diketiminate) catalysts (at $T = 25$ °C) was not observed for our complex, even though the ancillary ligand in $L^{SiMe2Ph}Sn(OCPh_3)$ also is large. Notably, only a slight heterotactic bias for the polymerization of LA was observed using a related monomeric Sn(II) catalyst that incorporates the same bulky β-diketiminate as in the Zn example.[13] These results may be a consequence of the stereochemically active lone pair of electrons on Sn(II), although more detailed mechanistic information is required to fully understand the source (or absence) of stereocontrol in these and related systems. Finally, polymerization of L-lactide using $L^{SiMe2Ph}Sn(OCPh_3)$ or $L^{SiMe2Ph}Sn(OCPh_3)$/BnOH yielded stereochemically pure poly-L-lactide (by ^1H NMR spectroscopy), indicating no epimerization of the monomer or polymer under the reaction conditions (i.e., toluene, 80 °C).

Kinetic Studies. Rates of polymerization of LA at 80 °C in toluene solution were monitored by IR spectroscopy using a ReactIR instrument fitted with an immersible diamond probe. A representative stack plot showing the change in IR spectra with LA conversion is shown in Figure 5. The polymerization was monitored by following the decrease in the absorbance of the band at 1242 cm^{-1}, which is present in LA and absent in PLA. Bands at 1185 and 934 cm^{-1}, corresponding to PLA and LA, respectively, were also monitored in some initial experiments, but better reproducibility between runs was obtained with the 1242 cm^{-1} data.[25] Using $L^{SiMe2Ph}Sn(OCPh_3)$ with 1.0 equiv of BnOH as the catalyst/initiator and between 50 and 400 equiv of LA, the

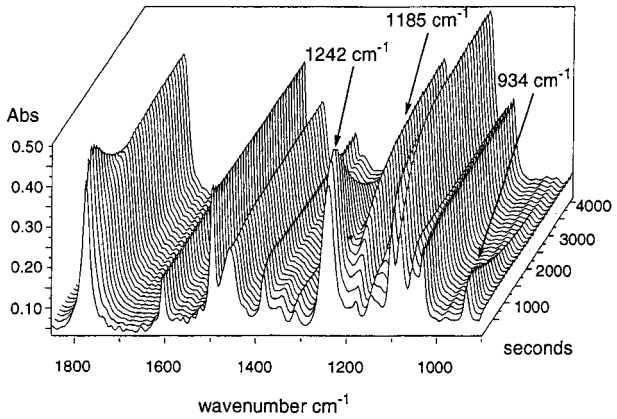

Figure 5. Representative plot of IR spectra vs time for a polymerization of DL-lactide by $L^{SiMe2Ph}Sn(OCPh_3)$ with added BnOH. Polymerization conditions: $[L^{SiMe2Ph}Sn(OCPh_3)]_0 = [BnOH]_0 = 0.005$ M, $[LA]_0 = 1.0$ M, toluene, 80 °C.

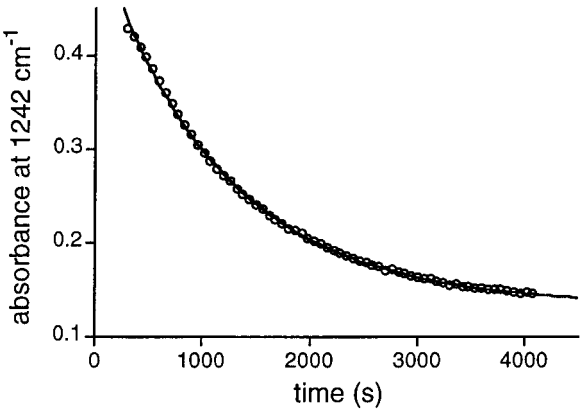

Figure 6. Representative plot of the IR absorbance at 1242 cm^{-1} vs time for the polymerization of DL-lactide by $L^{SiMe2Ph}Sn(OCPh_3)$ with added BnOH. The polymerization conditions are the same as Figure 5. The curve depicts a fit to the equation for first-order decay: $abs_t = (abs_0 - abs_\infty)\exp(-k_{app}t) + abs_\infty$, affording $k_{app} = (8.68 \pm 0.08) \times 10^{-4}$ s^{-1}, $abs_0 = 0.529 \pm 0.02$, and $abs_\infty = 0.1338 \pm 0.007$.

reaction displayed a clean first-order dependence on the LA concentration (Figure 6); without added BnOH a more complicated and difficult to interpret dependence on [LA] was found.

To measure the order in the Sn(II) reagent, polymerizations of 1.0 M LA in toluene at 80 °C were performed over a nearly 10-fold range of initial concentrations of $L^{SiMe2Ph}Sn(OCPh_3)$ (0.025−0.2 M) with equimolar BnOH present in each run. Measurements of the pseudo-first-order rate constant k_{app} at each $[Sn]_0$ (where "Sn" refers to $L^{SiMe2Ph}Sn(OCPh_3)$) were made in triplicate (Table S1), and a standard deviation was calculated for each measurement.[26] A plot of $\ln(k_{app})$ vs $\ln[Sn]_0$ (Figure 7) can be fit with a line that has a slope of 0.33 ± 0.02.[27] Thus, the rate law for the polymerization is described by eq 1.

$$-\frac{d[LA]}{dt} = k_{app}[LA] = k'[Sn]_0^{0.33\pm0.02}[LA] \quad (1)$$

The observed fractional order in precatalyst concentration suggests that, unlike the starting $L^{SiMe2Ph}Sn(OCPh_3)$, the catalytically active species aggregate and that the aggregate(s) is (are) less reactive for propagation.[28] Information on the nature of the aggregated species may be extracted from the kinetic data by

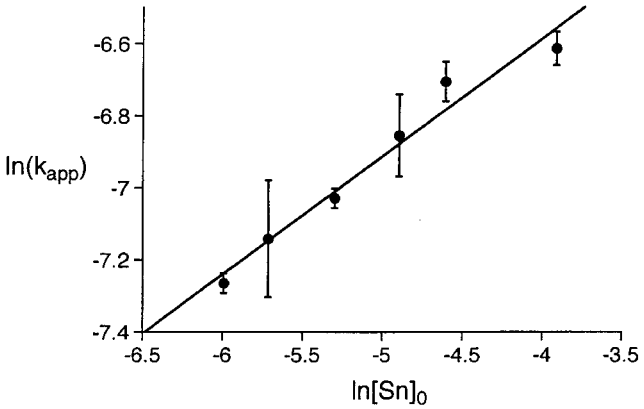

Figure 7. Plot of $\ln(k_{app})$ vs $\ln[Sn]_0$, where "Sn" refers to $L^{SiMe2Ph}Sn(OCPh_3)$. Polymerization conditions: $[Sn]_0 = [BnOH]_0$, $[LA]_0 = 1.0$ M, toluene, 80 °C. All measurements of k_{app} were made in triplicate, and the error bars on $\ln(k_{app})$ values correspond to one standard deviation. The slope of the indicated line is 0.33 ± 0.02 (ref 27).

following a previously described analysis.[29,30] The assumption that a single aggregate equilibrates with a mononuclear active species and that propagation occurs only from the latter is central to this treatment. This situation is described by eqs 2 and 3,

$$(P_n)_m \overset{K_{da}}{\rightleftharpoons} m P_n \tag{2}$$

$$P_n + LA \xrightarrow{k_{prop}} P_{n+1} \tag{3}$$

where P_n is a metal-capped polymer chain with a degree of polymerization n, $(P_n)_m$ is the aggregate of metal-capped polymer chains, and m is the aggregation number (restricted to an integer value). A simple kinetic expression may be derived from this scheme with the assumptions that (a) K_{da} is very small, that is, $[P_n] \ll [(P_n)_m]$ (essentially all polymerizing chains are aggregated at equilibrium), and (b) equilibration between the aggregated and unaggregated species is fast relative to propagation. The expression

$$k_{app} = \frac{k_{prop} K_{da}^{1/m}}{m^{1/m}} [Sn]_0^{1/m} \tag{4}$$

results from this analysis, and according to the natural logarithmic form of this equation, the slope of the experimental plot of $\ln(k_{app})$ vs $\ln[Sn]_0$ gives the inverse of the aggregation number m. We thus obtain $m = 3$ but also consider possible bracketing values of 2 or 4 in our analysis. To solve for k_{prop} and K_{da}, an alternate expression may be used (eq 5).[31]

$$k_{app}^{1-m} = \frac{-m k_{prop}^{1-m}}{K_{da}} + k_{prop} k_{app}^{-m} [Sn]_0 \tag{5}$$

For the appropriate value of m, a plot of k_{app}^{1-m} vs $k_{app}^{-m}[Sn]_0$ will be linear, and k_{prop} and K_{da} can be calculated from the slope and intercept. Plots of eq 5 with $m = 2$, 3, or 4 appear in Figure S4. While the data for $m = 2$ or 3 cannot be reasonably fit to a line, such a fit may be applied to the $m = 4$ plot.[32] This aggregation number of 4 is different from the value of 3 implied by the order in $[Sn]_0$ (Figure 7), suggesting that the assumptions made in the analysis, in particular the supposition of only one aggregated form, may be too simplistic. Notwithstanding this ambiguity, from the fit for $m = 4$ we find $k_{prop} = 0.43$ M^{-1} s^{-1} and $K_{da} = 2.9 \times 10^{-8}$ M^3.

We can now draw interesting kinetic comparisons with data reported previously for the polymerization of LA by $Sn(OBu)_2$.[9] Although measured values of k_{app} differ by a factor of ~4 (at $[Sn]_0 \approx 0.005$ M, $k_{app} = 3.6 \times 10^{-3}$ s^{-1} for $Sn(OBu)_2$ in THF vs $k_{app} = 8.9 \times 10^{-4}$ s^{-1} for $L^{SiMe2Ph}Sn(OCPh_3)$ in toluene, both at 80 °C), the more mechanistically meaningful propagation rate constants for the two systems are essentially the same ($k_{prop} = 0.5$ M^{-1} s^{-1} for $Sn(OBu)_2$ vs 0.43 M^{-1} s^{-1} for $L^{SiMe2Ph}Sn(OCPh_3)$). The difference in k_{app} values reflects differences in aggregation of active chains, K_{da} and/or m, but quantitative comparisons of these parameters between the two systems are difficult to make with the data currently available. Nevertheless, changing the nature of the catalyst appears to most significantly affect aggregation, not propagation, an important mechanistic conclusion that may not be obvious simply by comparing commonly measured k_{app} values.

Summary and Conclusions

Monomeric Sn(II) alkoxide complexes of bulky amidinate ligands, $[L^{SiMe2Ph}]^-$ and $[L^{SiMe3}]^-$, were synthesized and structurally characterized. NMR data showed that monomeric structures observed in the solid state are retained in solution. These complexes polymerize lactide in toluene at 80 °C. While variation in the alkyl silyl moieties of the amidinate did not significantly affect the solid-state structure of the complexes, catalytic behavior was influenced, with respect to polymerization control and initiation efficiency. Accordingly, the detailed LA polymerization activity of $L^{SiMe2Ph}Sn(OCPh_3)$ in the presence of 1.0 equiv of an exogenous alcohol was investigated. The use of an added small exogenous alcohol resulted in a marked improvement in the control of the polymerization of LA by $L^{SiMe2Ph}Sn(OCPh_3)$. Monitoring the $L^{SiMe2Ph}Sn(OCPh_3)$/BnOH mediated LA polymerization by in situ IR spectroscopy, the reaction was found to be first order in [LA] and 0.33 ± 0.02 in precatalyst concentration. The fractional order in catalyst indicates that there is a preequilibrium between a less active aggregated form of the growing polymer chain and a more active unaggregated form. Applying a model that assumes that there is only one inactive aggregated form, we estimated the equilibrium constant, K_{da}, and the propagation rate constant of the unaggregated form, k_{prop}. Comparing k_{app} and k_{prop} for $L^{SiMe2Ph}Sn(OCPh_3)$/BnOH and $Sn(OBu)_2$, we find that while $Sn(OBu)_2$ is a faster catalyst, the divergent reactivity is due to a difference in aggregation behavior of the active chains rather than a difference in the inherent rate of monomer incorporation. These results point to the importance of aggregation in understanding catalyst reactivity, with key implications for future efforts aimed at designing more effective catalysts for cyclic ester polymerizations.

Experimental Section

General Procedures. Air-sensitive reactions were performed in a M. Braun glovebox under an N_2 atmosphere or using standard Schlenk and vacuum line techniques. Toluene, pentane, THF, TMEDA, and diethyl ether were distilled from Na/benzophenone. Hexamethyldisiloxane was distilled from CaH_2. Benzonitrile, $NH(SiMe_3)_2$, and $NH(SiMe_2Ph)_2$ were vacuum-distilled from 3 Å molecular sieves. DL-Lactide (Aldrich) was recrystallized from dry toluene and then sublimed.

n-BuLi (Acros) was titrated using Ph_2CHCO_2H prior to use.[33] NaHMDS (Aldrich) and anhydrous $SnCl_2$ (Alfa Aesar) were used without further purification. Ph_3COH (Aldrich) was recrytallized from dry Et_2O prior to use. $L^{SiMe3}Na(Et_2O)$[19] was prepared following a literature procedure. NMR spectra were recorded using a Varian VXR-500, VXR-300, or VI-300 spectrometer. ^{119}Sn NMR spectra were referenced externally to Ph_2SnCl_2 (25% w/w in $CDCl_3$, δ −27.0). Molecular weights (M_n and M_w) and polydispersity indices (PDI = M_w/M_n) were determined by size exclusion chromatography (SEC) with respect to polystyrene standards. Samples were analyzed at 40 °C using a Waters high-pressure liquid chromatograph equipped with three Jordi poly(divinylbenzene) columns of 10^4, 10^3, and 500 Å pore sizes and a Waters 2410 refractive index detector. $CHCl_3$ was eluted at a flow rate of 1.0 mL/min.

$L^{SiMe3}Sn(OCPh_3)$. $Na(Et_2O)L^{SiMe3}$ (2.90 g, 7.29 mmol) was dissolved in THF (50 mL). $SnCl_2$ (1.38 g, 7.28 mmol) was added, and the resulting solution was stirred at room temperature for 90 min. LiHMDS (1.22 g, 7.29 mmol) was dissolved in THF (10 mL) and added to the reaction. The suspension was stirred at room temperature for 16 h. The suspension was filtered, and the filtrate was concentrated in vacuo fully to obtain a pale yellow solid that was extracted into Et_2O (90 mL) overnight. LiCl and NaCl were removed by filtration, the filtrate was concentrated in vacuo, and $L^{SiMe3}Sn[N(SiMe_3)_2]$ was isolated as a viscous pale yellow oil (2.956 g, 75%). ^1H NMR (C_6D_6): δ 6.92−7.18 (m, 5 H), 0.45 (s, 18 H, amide −NSi(CH_3)$_3$), −0.05 (s, 18 H, amidinate −NSi(CH_3)$_3$). A solution of $L^{SiMe3}Sn[N(SiMe_3)_2]$ (2.956 g, 5.44 mmol) in toluene (30 mL) was added to a solution of Ph_3COH(1.42 g, 5.45 mmol) in toluene (20 mL). The solution was stirred at room temperature overnight, and then solvent was removed in vacuo. The tacky tan solid was extracted into Et_2O (50 mL). A small amount of fine white powder precipitated out overnight and was filtered off. The resulting pale yellow solution was concentrated in vacuo to 15 mL. Pentane (15 mL) and HMDSO (4 mL) were added, and the solution was placed in the −35 °C freezer. Colorless crystals formed overnight (1.95 g, 56%). ^1H NMR (C_6D_6): δ 6.96−7.84 (m, 20 H), −0.11 (s, 18 H, Si(CH_3)$_3$). ^{13}C NMR (C_6D_6): δ 183.53, 152.55, 142.82, 129.37, 129.26, 126.95, 126.71, 84.55, 1.65. ^{119}Sn NMR (0.1 M in C_6D_6): δ −54.16. Anal. Calcd for $C_{32}H_{38}N_2OSi_2Sn$: C, 59.91; H, 5.97; N, 4.37. Found: C, 59.61; H, 5.92; N, 4.39.

$(L^{SiMe3})_2Sn$. $SnCl_2$ (348 mg, 1.84 mmol) was added to a solution of $Na(Et_2O)L^{SiMe3}$ (1.33 g, 3.64 mmol) in THF (15 mL). The suspension was stirred at room temperature for 16 h, and then the solvent was removed in vacuo. The tacky yellow-orange solid was dissolved/suspended in toluene (8 mL) and pentane (8 mL). The suspension was stirred for 4 h and then filtered. The resulting orange solution was concentrated in vacuo to 4 mL. Colorless crystals (552 mg, 49%) formed when the solution was cooled to −35 °C. ^1H NMR (C_6D_6): δ 6.96−7.18 (m, 10 H), 0.09 (s, 36 H, Si(CH_3)$_3$). ^{119}Sn NMR (0.02 M in C_6D_6): δ −244.58. Anal. Calcd for $C_{26}H_{46}N_4Si_4Sn$: C, 48.36; H, 7.18; N, 8.68. Found: C, 47.82; H, 6.86; N, 8.58.

$L^{SiMe2Ph}Li(TMEDA)$. A solution of $HN(SiMe_2Ph)_2$ (4.8 mL, 16.6 mmol) in hexanes (80 mL) was cooled to 0 °C and treated with *n*-BuLi (9.3 mL, 1.63 M, 15.2 mmol). The colorless solution was stirred at 0 °C for 45 min and room temperature for 15 min. The solution was cooled to 0 °C, and benzonitrile (1.54 mL, 15.1 mmol) was added. White precipitate formed midway through the addition. The suspension was stirred at 0 °C for 90 min. The solution became homogeneous upon addition of toluene (20 mL) and with gentle heating. The solution was heated under N_2 below its reflux temperature for 16 h. TMEDA (3.0 mL, 19.9 mmol) was added, and the solution was stirred at room temperature for 1 h. The solvent was removed in vacuo, and the product was crystallized from pentane (6.20 g, 80%). ^1H NMR (C_6D_6): δ 6.94−7.69 (m, 15 H), 1.85 (s, 12 H, NCH_3), 1.62 (s, 4 H, CH_2N), 0.18 (s, 12 H, Si(CH_3)$_2$. Anal. Calcd for $C_{29}H_{43}LiN_4Si_2$: C, 68.20; H, 8.49; N, 10.97. Found: C, 67.01; H, 8.33; N, 10.44.

$L^{SiMe2Ph}Sn(OCPh_3)$. $L^{SiMe2Ph}Li$(TMEDA) (949 mg, 1.85 mmol) was dissolved in THF (12 mL) and added to $SnCl_2$(352 mg, 1.86 mmol). The reaction was stirred at room temperature for 3 h. A solution of LiHMDS (311 mg, 1.86 mmol) in THF (4 mL) was added, and the reaction was stirred at room temperature for 17 h. The solvent was removed in vacuo. The resulting solid was extracted into ether (15 mL) overnight. The precipitate was filtered off, and the solvent was removed in vacuo. The product, crude $L^{SiMe2Ph}Sn[N(SiMe_3)_2]$, was dissolved in toluene (15 mL) and treated with a solution of Ph_3COH (410 mg, 1.57 mmol) in toluene (2 mL). The solution was stirred at room temperature for 18 h. A small amount of white precipitate had formed and was filtered off. The solvent was removed in vacuo, and the product was crystallized from 5:1 Et_2O/HMDSO (733 mg, 61%). ^1H NMR (C_6D_6): δ 6.71−7.75 (m, 30 H), 0.08 (s, 6 H), 0.04 (s, 6 H). ^{13}C NMR ($C_6D_5CD_3$) (including one toluene triplet between 128.5 and 129.3): δ 184.04, 152.05, 141.67, 139.20, 134.06, 129.27, 129.15, 128.98, 128.84, 128.71, 128.52, 128.00, 126.52, 126.41, 84.44, −0.075, −0.328. ^{119}Sn NMR (0.1 M in $C_6D_5CD_3$): δ −70.33. Anal. Calcd for $C_{42}H_{42}N_2OSi_2Sn$: C, 65.88; H, 5.53; N, 3.66. Found: C, 65.37; H, 5.57; N, 3.65.

$(L^{SiMe2Ph})_2Sn$. $L^{SiMe2Ph}Li$(TMEDA) (404 mg, 0.791 mmol) was dissolved in THF (8 mL) and added to $SnCl_2$ (75 mg, 0.396 mmol). The suspension was stirred at room temperature for 7 h and then concentrated in vacuo fully. The solid was extracted into Et_2O (12 mL) overnight and then filtered. The filtrate was concentrated, and HMDSO was added. Crystals of $(L^{SiMe2Ph})_2Sn$ (228 mg, 64%) formed after the solution was cooled to −35 °C. ^1H NMR (C_6D_6): δ 6.64−7.51 (m, 30 H), 0.17 (s, 24 H). ^{119}Sn NMR (0.02 M in C_6D_6): δ −226.97. Anal. Calcd for $C_{46}H_{54}N_4Si_4Sn$: C, 61.80; H, 6.09; N, 6.27. Found: C, 60.53; H, 6.17; N, 6.23. Difficulty in obtaining an exact microanalysis has been reported for another Sn(II) bis(amidinate) complex.[18]

X-ray Crystallography. Single crystals of $L^{SiMe3}Sn(OCPh_3)$, $L^{SiMe2Ph}Sn(OCPh_3)$, $(L^{SiMe3})_2Sn$, and $(L^{SiMe2Ph})_2Sn$ were attached to glass fibers and mounted on a Siemens SMART system for data collection at 173 (2) K. An initial set of cell constants was calculated from three sets of 20 frames. These initial sets of frames were oriented such that orthogonal wedges of reciprocal space were surveyed; orientation matrices were calculated from 150 to 320 reflections. Final cell constants were collected from a data set that did not exceed 8192 strong reflections from the actual data collection after integration. A randomly oriented region of reciprocal space was surveyed to the extent of 1.3 hemispheres to a resolution of 0.77 Å. Three major swaths of frames were collected in 0.30° steps in ω. Space groups were determined on the basis of systematic absences and intensity statistics.[34] Successful direct-methods solutions were calculated which provided most of the non-hydrogen atoms from the E-maps.[35] Several full-matrix least-squares/difference Fourier cycles were performed to locate the remainder of the non-hydrogen atoms. All non-hydrogen atoms were refined with anisotropic displacement parameters. All hydrogen atoms were placed in ideal positions and refined as riding atoms with individual (or group if appropriate) isotropic displacement parameters. Selected crystallographic data are presented in Table 1, and the CIF files for all four structures are included as Supporting Information.

General Polymerization Procedure. In the glovebox, a screw-cap vessel was charged with LA (216 mg), a toluene stock solution of the Sn catalyst, and a toluene stock solution of BnOH (if added) to yield a 1.0 M solution of LA and the desired ratio of LA to catalyst. The Teflon screw-cap was tightly affixed, and the vessel was brought out of the glovebox and heated, with stirring, in an 80 °C bath. After an interval of time, the screw-cap was removed, and a few drops of the solution were removed and added to an NMR tube containing $CDCl_3$. This sample was immediately frozen in liquid N_2, and after thawing, a ^1H NMR spectrum of the solution was recorded. The remainder of the polymerization solution was added to heptane to precipitate the solute(s), dried (~80 °C, vacuum, 6 h), and subjected to analysis by size exclusion chromatography.

Kinetics. Reaction rates were monitored by following changes in the IR spectra using a ReactIR 1000 or ReactIR 4000 instrument from ASI Applied Systems. In the glovebox, the reaction vessel was charged with LA (288 mg) and the

appropriate amount of toluene stock solutions of L^{SiMe2}-$PhSnOCPh_3$ and BnOH to give a 1.0 M solution of LA and the desired $[LA]_0/[L^{SiMePh}SnOCPh_3]_0$ ratio. The reaction vessel was attached to the IR probe via a ground-glass joint, and the probe was brought out of the glovebox and attached to the ReactIR instrument. The reaction vessel was then submerged in a temperature-controlled 80 °C bath. The full dissolution of LA in toluene at 80 °C required 3−5 min; accordingly, IR spectra recorded in the first 5 min were not included in the data analysis. The absorbance at 1242 cm^{-1}, a fingerprint band present in LA and absent in PLA, was monitored for 5 half-lives. Full conversion, as observed by IR spectroscopy, was confirmed by ^1H NMR spectroscopy for some kinetic runs. All measurements of k_{app} were made in triplicate, and the error bars on k_{app} values correspond to one standard deviation. Nonlinear and linear unweighted curve fits were performed using Kaleidagraph.

Acknowledgment. We thank the NSF (CHE9975357) for support of this work and Dr. Brendan O'Keefe for helpful discussions.

Supporting Information Available: Representations of the crystal structures of $L^{SiMe3}SnOCPh_3$ and $L^{SiMe2Ph}SnOCPh_3$ (Figures S1 and S2), the homonuclearly decoupled ^1H NMR spectrum of a PLA sample (Figure S3), listing of measured k_{app} values (Table S1), plots of $k_{app}{}^{1-m}$ vs $k_{app}{}^{-m}[Sn]_0$ for varying m values (Figure S4), and full X-ray structural information. This material is available free of charge via the Internet at http://pubs.acs.org.

References and Notes

(1) O'Keefe, B. J.; Hillmyer, M. A.; Tolman, W. B. *J. Chem. Soc., Dalton Trans.* **2001**, 2215.
(2) Amass, W.; Amass, A.; Tighe, B. *Polym. Int.* **1998**, *47*, 89.
(3) Drumright, R. E.; Gruber, P. R.; Henton, D. E. *Adv. Mater.* **2000**, *12*, 1841.
(4) Tullo, A. *Chem. Eng. News* **2000** *Jan 17* (no. 3), 13.
(5) For leading references on the use of $Sn(Oct)_2$ for cyclic ester polymerization, see: (a) Takayanagi, H.; Kobayashi, T.; Masuda, T.; Shinoda, H. Eur. Patent EP 88-306393 19880713, 1989; *Chem. Abstr.* **1989**, *110*, 135964. (b) Duda, A.; Penczek, S. *Macromolecules* **1990**, *23*, 1636. (c) Nijenhuis, A. J.; Grijpma, D. W.; Pennings, A. J. *Macromolecules* **1992**, *25*, 6419. (d) Kricheldorf, H. R.; Kreiser-Saunders, I.; Boettcher, C. *Polymer* **1995**, *36*, 1254.
(6) Kowalski, A.; Duda, A.; Penczek, S. *Macromol. Rapid Commun.* **1998**, *19*, 567.
(7) Kowalski, A.; Duda, A.; Penczek, S. *Macromolecules* **2000**, *33*, 689.
(8) Kowalski, A.; Duda, A.; Penczek, S. *Macromolecules* **2000**, *33*, 7359.
(9) Kowalski, A.; Libiszowski, J.; Duda, A.; Penczek, S. *Macromolecules* **2000**, *33*, 1964.
(10) *The Chemistry of Tin;* Harrison, P. G., Ed.; Blackie: Glasgow, 1989; p 25.
(11) Cetinkaya, B.; Gümrükcü, I.; Lappert, M. F.; Atwood, J. L.; Rogers, R. D.; Zaworotko, M. J. *J. Am. Chem. Soc.* **1980**, *102*, 2088.
(12) Fjeldberg, T.; Hitchcock, P. B.; Smith, S. J.; Thorne, A. J. *J. Chem. Soc., Chem. Commun.* **1985**, 939.
(13) Dove, A. P.; Gibson, V. C.; Marshall, E. L.; White, A. J. P.; Williams, D. J. *Chem. Commun.* **2001**, 283.
(14) Reviews: (a) Barker, J.; Kilner, M. *Coord. Chem. Rev.* **1994**, *133*, 219. (b) Edelmann, F. T. *Coord. Chem. Rev.* **1994**, *137*, 403. Selected recent examples of *N,N′*-bis(trimethylsilyl)-benzamidinate complexes: (c.) Flores, J. C.; Chien, J. C. W.; Rausch, M. D. *Organometallics* **1995**, *14*, 1827. (d) Hagadorn, J. H.; Arnold, J. *Organometallics* **1998**, *17*, 1355. (e) Brussee, E. A. C.; Meetsma, A.; Hessen, B.; Teuben, J. H. *Chem Commun.* **2000**, 497. (f) Aubrecht, K. B.; Chang, K.; Hillmyer, M. A.; Tolman, W. B. *J. Polym. Sci., Part A: Polym. Chem.* **2001**, *39*, 284.
(15) Kilimann, U.; Noltemeyer, M.; Edelmann, F. T. *J. Organomet. Chem.* **1993**, *443*, 35.
(16) Zhou, Y.; Richeson, D. S. *J. Am. Chem. Soc.* **1996**, *118*, 10850.
(17) Foley, S. R.; Yap, G. P. A.; Richeson, D. S. *Organometallics* **1999**, *18*, 4700.
(18) Foley, S. R.; Zhou, Y.; Yap, G. P. A.; Richeson, D. S. *Inorg. Chem.* **2000**, *39*, 924.
(19) Wedler, M.; Knösel, F.; Noltemeyer, M.; Edelmann, F. T. *J. Organomet. Chem.* **1990**, *388*, 21.
(20) (a) Harris, D. H.; Lappert, M. F. *J. Chem Soc., Chem. Commun.* **1974**, 895. (b) Braunschweig, H.; Chorley, R. W.; Hitchcock, P. B.; Lappert, M. F. *J. Chem. Soc., Chem. Commun.* **1992**, 1311.
(21) The chemical shift of a 0.08 M solution of $L^{SiMe2Ph}SnOCPh_3$ in d_8-toluene only decreases from δ −69.0 to δ −70.7 as the probe temperature is raised from ambient temperature to 80 °C. Changes in ^{119}Sn chemical shifts for changes in aggregation from monomer to dimer are on the order of 100 ppm. See: Kennedy, J. D. *J. Chem. Soc., Perkins Trans. 2* **1977**, 242.
(22) The concept of using an alcohol as a chain transfer agent in the polymerization of cyclic compounds with metal alkoxide catalysts has been applied in many examples of lactide and other cyclic ester polymerizations (refs 6−9) and in the "immortal" polymerizations described by in: Aida, T.; Inoue, S. *Acc. Chem. Res.* **1996**, *29*, 39.
(23) Thakur, K. A. M.; Kean, R. T.; Hall, E. S.; Doscotch, M. A.; Munson, E. J. *Anal. Chem.* **1997**, *69*, 4303.
(24) Chamberlain, B. M.; Cheng, M.; Moore, D. R.; Ovitt, T. M.; Lobkovsky, E. B.; Coates, G. W. *J. Am. Chem. Soc.* **2001**, *123*, 3229.
(25) The intense carbonyl band shifts only slightly upon opening of the ring (LA = 1775 cm^{-1}; PLA = 1760 cm^{-1}) so it was not followed in the kinetic analysis.
(26) The expression for calculating the standard deviation of a small data set was used. Skoog, D. A. *Principles of Instrumental Analysis*; Saunders College Publishing: Philadelphia, 1985; p 8.
(27) The error on the slope was estimated from the standard deviation of each k_{app} value and the expression for uncertainties in the coefficients of the equation for the line in Figure 7 when the uncertainty for each data point is not the same. Bevington, P. R. *Data Reduction and Error Analysis for the Physical Sciences*; McGraw-Hill: New York, 1969; p 116.
(28) Because we are monitoring propagation (loss of LA), rather than initiation, (conversion of the $L^{SiMe2Ph}SnOCPh_3$ precatalyst to the active catalyst), the observed fractional order in $[L^{SiMe2Ph}SnOCPh_3]_0$ cannot be due to a preequilibrium prior to initiation. In addition, initiation of polymerization is fast relative to propagation (as shown by the first-order kinetics in Figure 6).
(29) Szwarc, M.; Van Beylen, M. *Ionic Polymerization and Living Polymers*; Chapman and Hall: New York, 1993; Chapter 3.
(30) (a) Duda, A.; Penczek, S. *Macromol. Rapid Commun.* **1994**, *15*, 559. (b) Kowalski, A.; Duda, A.; Penczek, S. *Macromolecules* **1998**, *31*, 2114.
(31) Duda, A.; Penczek, S. *Makromol. Chem., Macromol. Symp.* **1991**, *47*, 127.
(32) While the fit in the $m = 4$ plot is better than that for $m = 3$, it is inherent to the nature of the exponential term in eq 5 that larger m values will result in improved linear correlations in plots of $k_{app}{}^{1-m}$ vs $[Sn]_0 k_{app}{}^{-m}$.
(33) Kofron, W. G.; Baclawski, L. M. *J. Org. Chem.* **1976**, *41*, 1879.
(34) SHELXTL-Plus V5.1 Siemens Industrial Automation, Inc., Madison, WI.
(35) SIR92, Atomare, A.; Cascarno, G.; Giacovazzo, C.; Gualardi, A. *J. Appl. Crystallogr.* **1993**, *26*, 343.

MA011873W